

Solid Solution $V_xFe_{1-x}[TCNE]_2 \cdot zCH_2Cl_2$ Room-Temperature Magnets

Konstantin I. Pokhodnya,^{†,‡} Elaine B. Vickers,[†] Michael Bonner,[†]
Arthur J. Epstein,[‡] and Joel S. Miller^{*,†}

Department of Chemistry, University of Utah, Salt Lake City, Utah 84112-0850, and
Departments of Chemistry and Physics, The Ohio State University,
Columbus, Ohio 43210-1106

Received April 19, 2004. Revised Manuscript Received May 20, 2004

A family of amorphous, solid-solution magnets of $V_xFe_{1-x}[TCNE]_2 \cdot zCH_2Cl_2$ (TCNE = tetracyanoethylene; $0 \leq x \leq 1$) composition has been characterized by IR spectrometry, elemental analysis, and magnetic measurements (ac and dc susceptibility). Substitution of Fe^{II} for V^{II} in $V[TCNE]_2 \cdot zCH_2Cl_2$ does not significantly alter the T_c for $x \geq 0.3$, which exceeds room temperature; however, H_{cr} is enhanced by over 2 orders of magnitude, indicating a large increase of random anisotropy. Hence, the magnetic properties of the room-temperature $V[TCNE]_2 \cdot zCH_2Cl_2$ magnet can be finely tuned via a synthetic chemistry methodology, making this material more amenable to future technologies.

Introduction

The reaction of $V(CO)_6$ and tetracyanoethylene (TCNE) in either dichloromethane or in the vapor phase forms a magnet of nominal $V[TCNE]_y \cdot zCH_2Cl_2$ ($y \approx 2$; $z \approx 0.3$;^{1a} $y \approx 2$; $z = 0$ ^{1b}) composition with a magnetic ordering temperature (T_c) exceeding room temperature. The latter chemical vapor deposition (CVD) methodology led to thin films of this $V[TCNE]_y$ magnet with enhanced air stability.^{1b} $V[TCNE]_y$ is a disordered, amorphous magnet with a small coercivity, H_{cr} , of ~ 7.4 and < 1 Oe at 5 K and room temperature, respectively.² Furthermore, $V[TCNE]_y$ films are magnetic semiconductors (room-temperature conductivity of $\sim 10^{-4}$ S/cm) and magnetotransport studies reveal that the electrons in valence and conducting bands are spin polarized, suggesting “spintronic” applications.³ Utilization of the reaction of TCNE with other first-row homoleptic metal carbonyls to form magnetic materials has only been

reported for $Fe[TCNE]_2 \cdot zCH_2Cl_2$ ($T_c = 100$ K).⁴ The reaction of TCNE and $Co_2(CO)_8$, albeit fast, does not lead to a magnetically ordered material.⁵ Nonetheless, due to the fast reaction of TCNE with $Co_2(CO)_8$, solid solutions of $V_xCo_{1-x}[TCNE]_2 \cdot zCH_2Cl_2$ composition exhibiting properties differing from those for $x = 0$ or 1 have been characterized. Substitution of Co^{II} for V^{II} for $x > 0.3$ in $V[TCNE]_y \cdot zCH_2Cl_2$, $V_xCo_{1-x}[TCNE]_2 \cdot zCH_2Cl_2$, does not significantly change T_c ; however, the 5 K H_{cr} is enhanced to 270 Oe, with the room temperature H_{cr} enhanced to ~ 15 Oe.⁵

The substitution of Fe^{II} for V^{II} with its significant magnetocrystalline anisotropy⁶ should lead to materials with enhanced coercivity and relatively high T_c values, as $Fe[TCNE]_2 \cdot zCH_2Cl_2$ has a T_c of 100 K. However, formation of $V_xFe_{1-x}[TCNE]_2 \cdot zCH_2Cl_2$ via eq 1 seemed unlikely due to the substantial difference in reaction rates in the synthesis of $V[TCNE]_y \cdot zCH_2Cl_2$, which forms instantaneously, and $Fe[TCNE]_2 \cdot zCH_2Cl_2$, which gradually forms after several days.⁴ It was therefore anticipated that $V[TCNE]_y$ would form rapidly, followed by slow formation of $Fe[TCNE]_2$. Nonetheless, with the goal of enhancing the coercivity needed for some spintronic⁷ and other applications, $V_xFe_{1-x}[TCNE]_2 \cdot zCH_2Cl_2$ ($0 < x < 1$) were sought and unexpectedly prepared from CH_2Cl_2 via eq 1. Herein we report the results of a study

* To whom correspondence should be addressed. E-mail: jsmiller@chem.utah.edu.

[†] University of Utah.

[‡] The Ohio State University.

(1) (a) Manriquez, J. M.; Yee, G. T.; McLean, R. S.; Epstein, A. J.; Miller, J. S. *Science* **1991**, *252*, 1415. Epstein, A. J.; Miller, J. S. In *Conjugated Polymers and Related Materials: The Interconnection of Chemical and Electronic Structure*, Proceedings of Nobel Symposium NS-81; Oxford University Press: New York, 1993; p 475. *La Chim. La Ind.* **1993**, *75*, 185, 257. Miller, J. S.; Yee, G. T.; Manriquez, J. M.; Epstein, A. J. In *Conjugated Polymers and Related Materials: The Interconnection of Chemical and Electronic Structure*, Proceedings of Nobel Symposium NS-81; Oxford University Press: New York, 1993; p 461; *La Chim. La Ind.* **1992**, *74*, 845. (b) Pokhodnya, K. I.; Epstein, A. J.; Miller, J. S. *Adv. Mater.* **2000**, *12*, 410.

(2) Pokhodnya, K. I.; Pejakovic, D.; Epstein, A. J.; Miller, J. S. *Phys. Rev. B* **2001**, *63*, 174408.

(3) Prigodin, V. N.; Raju, N. P.; Pokhodnya, K. I.; Miller, J. S.; Epstein, A. J. *Adv. Mater.* **2002**, *14*, 1230.

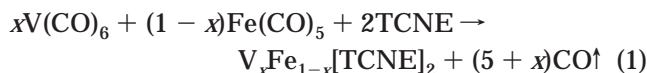
(4) Pokhodnya, K. I.; Petersen, N.; Miller, J. S. *Inorg. Chem.* **2002**, *41*, 1996.

(5) Pokhodnya, K. I.; Burtman, V.; Epstein, A. J.; Raebiger, J. W.; Miller, J. S. *Adv. Mater.* **2003**, *15*, 1211.

(6) Craik, D. *Magnetism Principles and Applications*; J. Wiley & Sons: New York, 1997; p 204 ff.

(7) Wolf, S. A. *J. Supercond.* **2000**, *13*, 195. Prinz, G. *Science* **1998**, *282*, 1660. Ohno, H.; Matsukura, F. *Solid State Commun.* **2001**, *117*, 179.

of V_xFe_{1-x}[TCNE]₂·zCH₂Cl₂ (0 < x < 1).



Experimental Section

Because of the extreme air and water sensitivities of the materials studied, all manipulations and reactions were performed in a Vacuum Atmospheres DriLab glovebox (<0.5 ppm O₂ and <1 ppm H₂O). CH₂Cl₂ was dried over two columns of activated alumina.⁸ V⁰(CO)₆ was prepared from [Et₄N][V⁻¹(CO)₆] via a literature preparation⁹ and was sublimed at 25 °C and 50 mTorr. TCNE was purified by sublimation at 85 °C and 50 mTorr to obtain a colorless, crystalline material.

In a typical preparation, appropriate equivalents of V(CO)₆ and Fe(CO)₅ (providing in total 0.16 mmol) were each dissolved in 5 mL of CH₂Cl₂, then combined and stirred. The combined metal solution was then added dropwise to a stirred, filtered solution of TCNE (0.32 mmol) in 10 mL of CH₂Cl₂, eq 1. The solution quickly turned dark with the evolution of CO and was stirred overnight with venting. The dark, amorphous product was filtered, washed with CH₂Cl₂, and dried (yield ~90%). Typical observed elemental analysis (calcd¹⁰) for V_xFe_{1-x}[TCNE]₂·zCH₂Cl₂ (x = 0; z = 1.00), C₁₃H₂FeN₈Cl₂: %C = 38.59 (39.34), %H = 0.54 (0.51), %N = 28.85 (28.23). (x = 0.14; z = 0.52), C_{12.52}H_{1.04}N₈V_{0.14}Fe_{0.86}Cl_{1.04}: %C = 42.57 (42.30), %H = 0.69 (0.29), %N = 31.32 (31.52), %V = 2.17 (2.01), %Fe = 13.53 (13.51). (x = 0.33; z = 0.57), C_{12.57}H_{1.14}N₈V_{0.33}Fe_{0.67}Cl_{1.14}: %C = 42.62 (42.08), %H = 0.94 (0.32), %N = 31.09 (31.23), %V = 4.82 (4.69), %Fe = 10.68 (10.43). (x = 0.51; z = 0.57), C_{12.57}H_{1.14}N₈V_{0.51}Fe_{0.49}Cl_{1.14}: %C = 42.59 (42.18), %H = 0.83 (0.32), %N = 31.36 (31.31), %V = 7.38 (7.26), %Fe = 7.69 (7.65). (x = 0.70; z = 0.92), C_{12.92}H_{1.84}N₈V_{0.70}Fe_{0.30}Cl_{1.84}: %C = 40.11 (40.13), %H = 0.49 (0.48), %N = 29.05 (28.98), %V = 9.08 (9.22), %Fe = 4.34 (4.33). (x = 0.89; z = 0.53), C_{12.53}H_{1.06}N₈V_{0.89}Fe_{0.11}Cl_{1.06}: %C = 43.28 (42.68), %H = 0.99 (0.30), %N = 31.86 (31.77), %V = 12.95 (12.86), %Fe = 1.72 (1.74). Since V[TCNE]₂·zCH₂Cl₂ is nonstoichiometric as y < 2,¹ V_xFe_{1-x}[TCNE]₂·zCH₂Cl₂, particularly as x → 1, might also have y < 2. Fits of the observed elemental analyses¹⁰ to V_xFe_{1-x}[TCNE]₂·zCH₂Cl₂, (0 ≤ x ≤ 1; y ≤ 2) are best for y = 2, as occurs for V_xCo_{1-x}[TCNE]₂·zCH₂Cl₂.⁵

Powder samples for magnetic measurements were loaded in airtight Delrin holders and packed with oven-dried quartz wool to prevent movement of the sample in the holder. The thread of the Delrin holder was vacuum greased as an additional protection from atmospheric oxygen due to the extreme air sensitivity of the materials. The temperature dependence of the DC magnetization was obtained by cooling in zero field and then data were collected on warming in 5 Oe external magnetic field using a Quantum Design MPMS-5XL 5 T SQUID magnetometer equipped with a reciprocating sample measurement system, low field option, and continuous low-temperature control with enhanced thermometry features. The onsets of the magnetic transition T_c's were obtained from an extrapolation of the low-field M(T) to the temperature at which M(T) → 0, as used in determining the T_c of V[TCNE]₂·zCH₂Cl₂^{1a,2} and V_xCo_{1-x}[TCNE]₂·zCH₂Cl₂.⁵ The AC magnetic susceptibility was measured in 3 Oe ac field (zero dc applied field) at 33, 100, and 1000 Hz. Phase-sensitive lock-in detection allowed both the in-phase (χ') and out-of-phase (χ'') linear susceptibilities to be extracted.

Thermogravimetric analysis (TGA) was performed on a TA Instruments TGA 2050 analyzer. Infrared spectra were obtained as Nujol mulls or KBr pellets on a Bruker Tensor 37

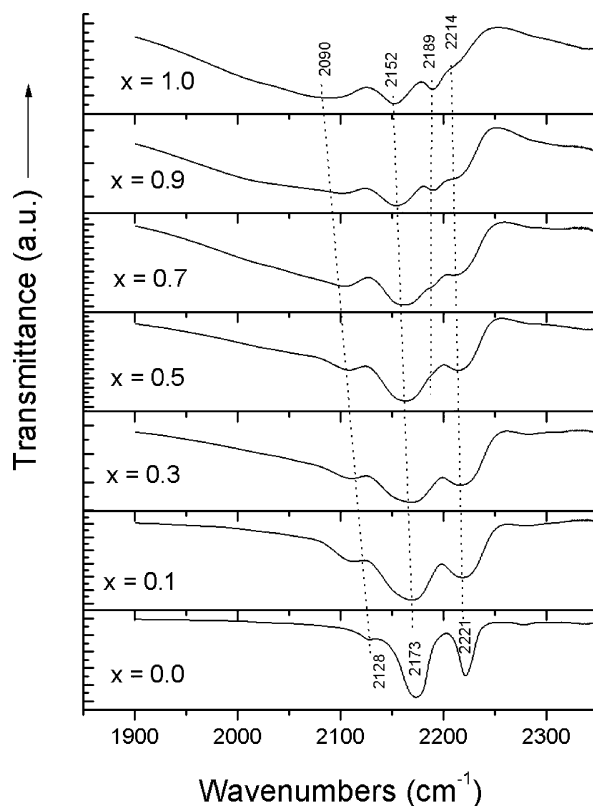


Figure 1. ν_{CN} IR spectra of V_xFe_{1-x}[TCNE]₂·zCH₂Cl₂ (0 ≤ x ≤ 1).

FTIR spectrometer (±1 cm⁻¹). Elemental analyses were performed by Complete Analysis Laboratories, Inc. of Parsippany, NJ.

Results and Discussion

The reaction of TCNE with V(CO)₆ and Fe(CO)₅ forms V[TCNE]₂·zCH₂Cl₂ and Fe[TCNE]₂·zCH₂Cl₂, respectively. The reaction with V(CO)₆ is instantaneous, whereas that with Fe(CO)₅ requires several days for completion.⁴ Hence, the formation of V_xFe_{1-x}[TCNE]₂·zCH₂Cl₂ (0 < x < 1) solid solutions via eq 1 seemed unlikely due to this difference in reaction rates; nonetheless, this reaction led to the instantaneous formation of a dark, amorphous solid, and IR and magnetic studies were evaluated to ascertain if a solid solution or physical mixture formed. Analysis of the fits of elemental analysis to compositions of the solid solutions showed that x was within experimental error (± 0.04) of the x used for the reactions.

Vibrational Spectroscopy. The $\nu_{C\equiv N}$ regions of the IR spectra of V_xFe_{1-x}[TCNE]₂·zCH₂Cl₂ (0 < x < 1) are consistent with formation of solid solutions. A physical mixture should consist of the superposition of the $\nu_{C\equiv N}$ absorptions for Fe[TCNE]₂·zCH₂Cl₂ (2221, 2173, 2128 cm⁻¹) and V[TCNE]₂·zCH₂Cl₂ (broad absorption at 2090 cm⁻¹ and three relatively narrow features at 2152, 2189, and 2214(sh) cm⁻¹).⁵ In contrast, solid solutions exhibit a family of spectra in which with decreasing of x (i) the broad 2090 cm⁻¹ feature becomes narrower and shifts toward 2128 cm⁻¹, and (ii) the 2152 and 2189 cm⁻¹ peaks merge together (for x > 0.5), forming a broad envelope with a diffuse maximum at 2173 cm⁻¹ (Figure 1). For Fe[TCNE]₂·zCH₂Cl₂, all peaks become narrower and a high-energy shoulder at 2178 cm⁻¹ of the 2172

(8) Pangborn, A. B.; Giardello, M. A.; Grubbs, R. H.; Rosen, R. K.; Timmers, F. J. *Organometallics* **1996**, *15*, 1518.

(9) Ellis, J. E.; Liu, X.; Selby, T. D.; Ghalsasi, P.; Miller, J. S. *Inorg. Synth.* **2004**, *34*, in press.

(10) Miller, J. S.; Kravitz, S. H.; Kirschner, S.; Ostrowski, P.; Nigrey, P. J. *J. Chem. Ed.* **1977**, *55*, 181. Miller, J. S.; Kravitz, S. H.; Kirschner, S.; Ostrowski, P.; Nigrey, P. J. *Quantum Chem. Prog. Exch.* **1977**, *10*, 341.

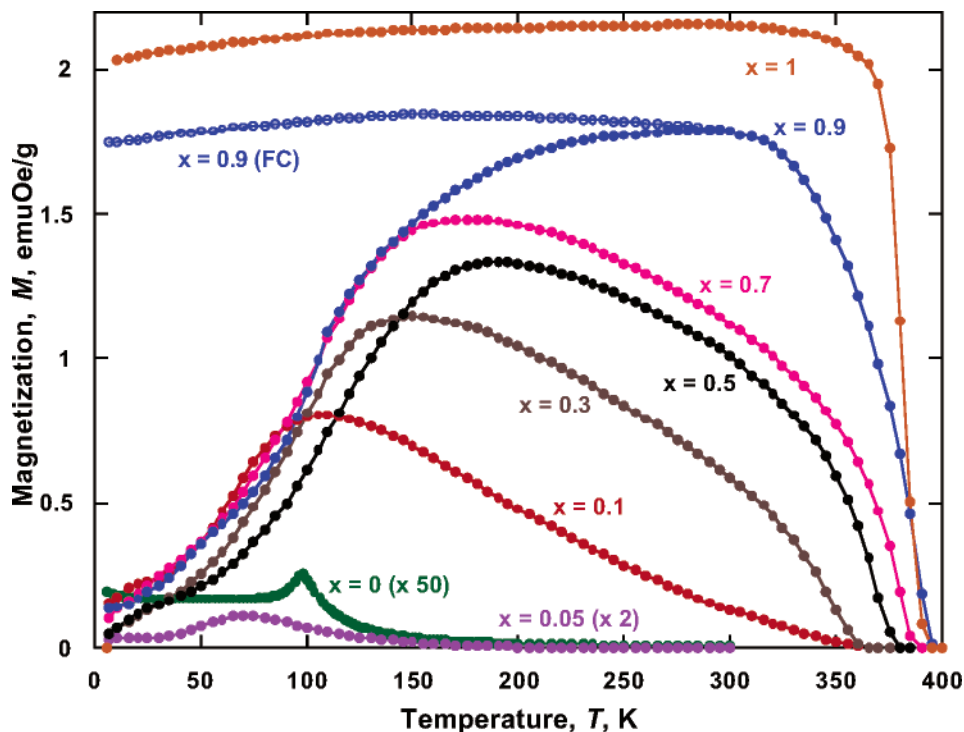


Figure 2. Temperature dependence of the zero field cooled (ZFC) and field cooled (FC) magnetization for $V_xFe_{1-x}[TCNE]_2 \cdot zCH_2Cl_2$. Data were collected in 5 Oe external magnetic field.

cm^{-1} absorption becomes more or less resolved depending upon the synthesis conditions. Finally, (iii) the feature at 2214 cm^{-1} shifts to 2221 cm^{-1} . The gradual transformation of absorptions with decreasing x is inconsistent with phase separation, implying that the correlated peaks have the same origin for $M[TCNE]_2 \cdot zCH_2Cl_2$ ($M = V, Fe$). Similar $\nu_{C=N}$ changes as a function of x were observed for $V_xCo_{1-x}[TCNE]_2 \cdot zCH_2Cl_2$.⁵ Hence, solid solutions of $V_xFe_{1-x}[TCNE]_2 \cdot zCH_2Cl_2$ composition form at variance with the slow reaction of $Fe(CO)_5$ and TCNE. This suggests that $V(CO)_6$ or a reaction intermediate(s) catalyzes this slow reaction.

Magnetic Studies. The 5–400 K temperature dependencies of the zero field cooled (ZFC) magnetization, $M(T)$, of $V_xFe_{1-x}[TCNE]_2 \cdot zCH_2Cl_2$ ($0 < x < 1$) solid solutions possess similar features and magnetically order above 350 K for $x \geq 0.3$ (Figure 2).¹¹ The 5 Oe magnetization is relatively small at low temperatures, increases upon warming, reaches a maximum, and then decreases with different slopes that increase with increasing x . The magnetization value at the maximum gradually decreases with decreasing x and approaches the value for $Fe[TCNE]_2 \cdot zCH_2Cl_2$ as $x \rightarrow 0$. The temperature of the maximum in $M(T)$, T_{max} , shifts from 280 to 70 K as x decreases from 0.9 to 0.05, but the onsets of the magnetic transitions are reduced only from 390 to 360 K for $x \geq 0.3$ with a shift to 200 K for $x = 0.05$. Field cooled (FC) $M(T)$ for $V[TCNE]_2 \cdot zCH_2Cl_2$ ($x = 1$) is essentially temperature-independent below ~ 350 K, and on further warming it drops abruptly as a magnetic

transition takes place with its onset at 390 K (Figure 2) in accord with that reported for $V[TCNE]_2 \cdot zCH_2Cl_2$.² It should be noted that the $M(T)$ of $V[TCNE]_2 \cdot zCH_2Cl_2$ and $Fe[TCNE]_2 \cdot zCH_2Cl_2$ have different behaviors at low fields (Figure 2), as the 5 Oe magnetization at 5 K differs by 2 orders of magnitude, despite both magnetically ordering at low temperatures.

Partial substitution of V^{II} in $V[TCNE]_2 \cdot zCH_2Cl_2$ by Fe^{II} introduces a substantial electronic and structural disorder that results in a significant irreversibility of magnetic properties as $M_{ZFC} \neq M_{FC}$ (Table 1; Figure 2). At 5 K, the FC magnetizations for the solid solutions are significantly (up to 70 times) higher than the ZFC values. In contrast, only a small irreversibility is observed for $V[TCNE]_2 \cdot zCH_2Cl_2$ ($< 10\%$ at 5 K). The irreversibility rapidly increases upon cooling below the bifurcation temperature, T_b , (the temperature at which M_{ZFC} deviates from M_{FC}), reminiscent of a spin-glass behavior.^{12a}

The temperature dependencies of the in-phase (χ') and out-of-phase (χ'') components of the AC susceptibility for $0.1 \leq x \leq 0.9$ solid solutions display broad peaks (Figure 3). The $\chi'(T)$ behavior is similar to that of $M(T)$ for $0.1 \leq x \leq 0.7$, as the temperature of the broad maximum, T_{max} , drops from ~ 160 to 115 K and the intensity decreases as x decreases from 0.9 to 0.1. For $x = 0.5$ above T_{max} , $\chi''(T)$ has a broad plateau at $225 < T < 300$ K that drops to zero at higher temperatures. The plateau widens with increasing x and the $\chi''(T)/\chi'(T_{max})$ ratio increases. This complex behavior suggests that at least two magnetic transitions occur in these materials. It should be noted that another peak is observed in both $\chi'(T)$ and $\chi''(T)$ at ≈ 20 K. This peak becomes more pronounced as Fe content increases, and a similar peak was observed in $Fe[TCNE]_2 \cdot zCH_2Cl_2$ and was assigned to a glassy transition.⁴

(11) The variation in T_c is attributed to difference in rates of temperature changes as well as small variations in the thermal stability of the materials, as TGA data indicate that decomposition starts by 350 K. This is a kinetic process; therefore $\sim 5\%$ increase in the transition onset temperature is due to a 20% increase of warming rate as reported in ref 2. Extrapolation of $M_s \rightarrow 0$ suggests $T_c \approx 410$ K.

Table 1. Summary of the IR and Magnetic Properties for $V_xFe_{1-x}[TCNE]_2 \cdot zCH_2Cl_2$

x	z^a	$T_c,^b$ K	$T_b,^c$ K	$M,^d$ emuOe/g (5 K)	$M_r,^e$ emuOe/g (5 K)	$H_{cr},^e$ Oe (5 K)	ν_{CN}, cm^{-1}
0	1.00	123	102	40.4	0.305	450	2221, 2173, 2128
0.03		157		34.5	3.76	1120	
0.05		145		34.8	2.99	970	
0.14	0.52	315	165	31.4	3.72	430	2219, 2170 broad, 2113 sh
0.33	0.57	359	225	30.6	7.18	275	2216, 2169 broad, 2111
0.51	0.57	376	260	28.1	12.2	265	2214, 2163 broad, 2108
0.73	0.73	386	300	27.0	11.6	215	2210, 2187 sh, 2162, 2105
0.89	0.89	394	>300	23.8	11.5	140	2206 sh, 2190, 2154, 2102
1.0	0.30	390 ^e	>300	23.9	3.6	9	2214 sh, 2189, 2152, 2090

^a Calculated from the elemental analysis data. ^b Obtained from an extrapolation of the low-field $M(T)$ to the temperature at which $M(T) \rightarrow 0$. ^c FC/ZFC bifurcation temperature. ^d M at 5 T, as saturation is not achieved. ^e Although an onset temperature of 390 K is higher than that reported in ref 2, it is within experimental error for $V[TCNE]_2 \cdot zCH_2Cl_2$.¹¹

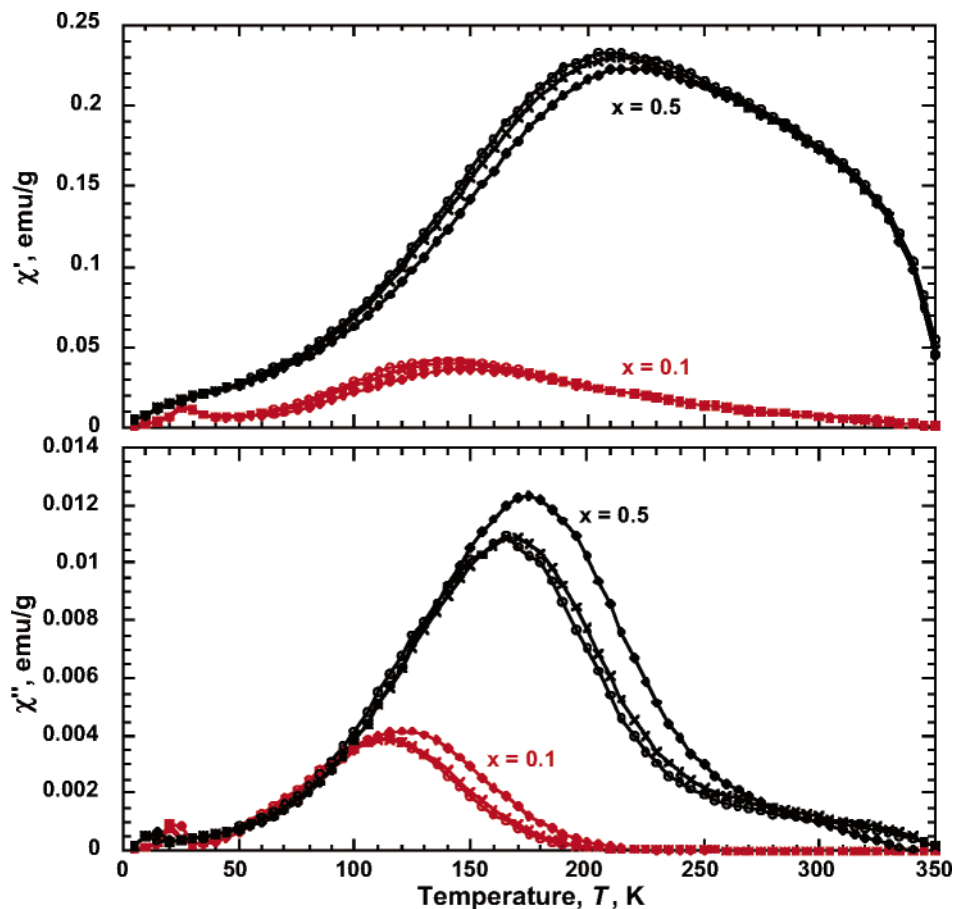


Figure 3. $\chi'(T)$ and $\chi''(T)$ for $V_xFe_{1-x}[TCNE]_2 \cdot zCH_2Cl_2$ ($x = 0.1, 0.5$) in $H_{ac} = 3$ Oe at 33 (○), 100 (×), and 1000 (◇) Hz.

The T_{max} in both $\chi'(T)$ and $\chi''(T)$ gradually increases with increasing frequency for all solid solutions, indicating the presence of time-dependent relaxation processes that are characteristic of spin-glasses.^{12b} The observed normalized T_{max} shift (ϕ) per a frequency (f) decade, defined as $\phi \equiv [\Delta T_{max} / T_{max} \Delta(\log f)]$, ranges from 0.03 to 0.05, which is low for superparamagnets.^{12c}

Because of the presence of Fe^{II} , an enhanced structural and electronic disorder in $V_xFe_{1-x}[TCNE]_2 \cdot zCH_2Cl_2$ is evident in the magnetization field dependence, $M(H)$ (Figure 4 inset). The $M(H)$ of $V[TCNE]_2 \cdot zCH_2Cl_2$ at 5 K reaches 95% of its saturation value at 2000 Oe, as previously reported.² In contrast, $M(H)$ of $Fe[TCNE]_2 \cdot zCH_2Cl_2$ at this temperature has an unusual constricted

shape with an inflection point at ± 10 kOe. Presumably the low magnetic response of $Fe[TCNE]_2 \cdot zCH_2Cl_2$ at $|H| < 10$ kOe could be explained by the presence of a macroscopic anisotropy field $H_a(T) \approx 10$ kOe created during cooling and having a structure similar to the domain pattern in the ferromagnetic phase; however, a metamagnetic or spin-flop transition cannot be excluded.¹³ The $M(H)$ for $Fe[TCNE]_2 \cdot zCH_2Cl_2$ at 50 kOe is twice that for $V[TCNE]_2 \cdot zCH_2Cl_2$ in accordance with twice the total spin of $S_{eff} = 1$; however, saturation is not achieved.

The different character of magnetization approaching saturation for $Fe[TCNE]_2 \cdot zCH_2Cl_2$ and $V[TCNE]_2 \cdot zCH_2Cl_2$ reveals itself in the $M(H)$ of the solid solutions

(12) Mydosh, J. A. *Spin Glasses*; Taylor & Francis: London, 1993. (a) p 69. (b) p 64. (c) p 67. (d) p 39.

(13) Girtu, M. A.; Wynn, C. M.; Zhang, J.; Miller, J. S.; Epstein, A. *J. Phys. Rev. B* **2000**, *61*, 492.

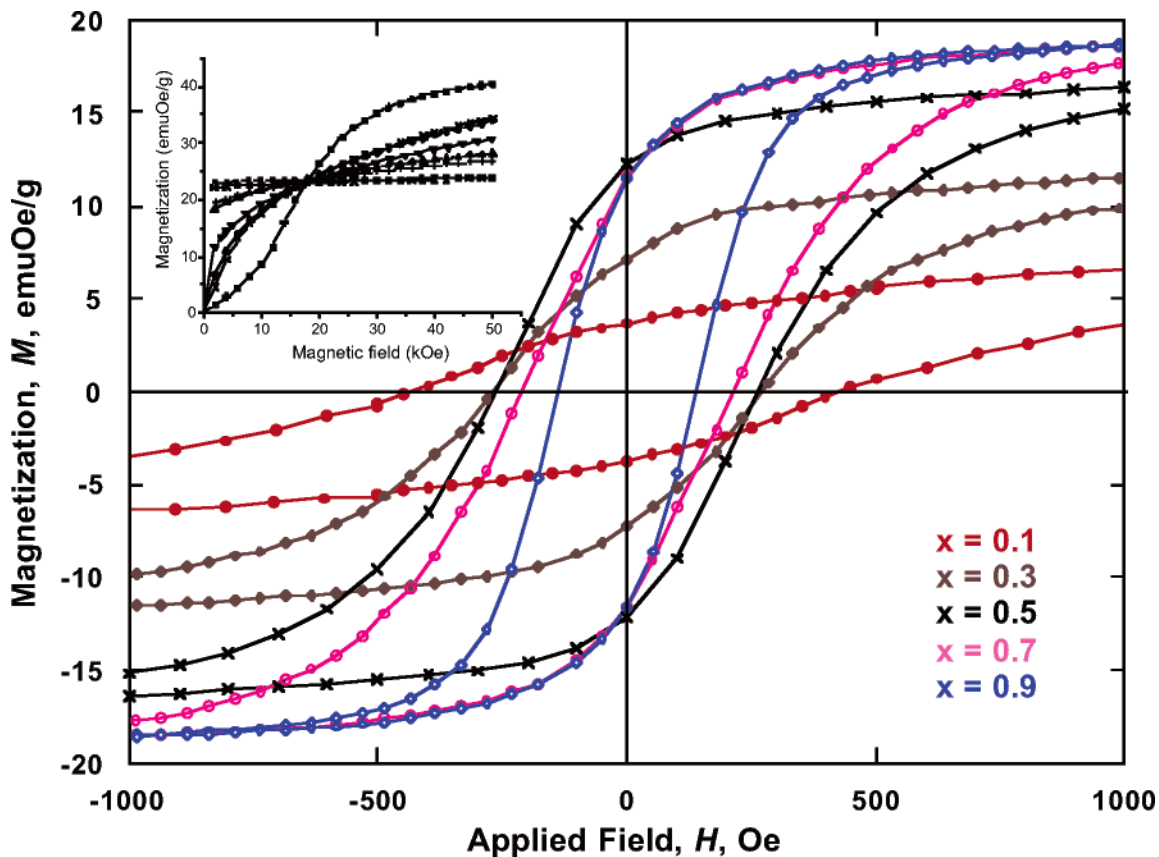


Figure 4. Hysteresis loops at 5 K for the $V_xFe_{1-x}[TCNE]_2 \cdot zCH_2Cl_2$ ($0.1 \leq x \leq 0.9$) solid solutions. Inset, 5 K $M(H)$ for $V_xFe_{1-x}[TCNE]_2 \cdot zCH_2Cl_2$: $x = 1$ (■); $x = 0.9$ (*); $x = 0.7$ (+); $x = 0.5$ (▲); $x = 0.3$ (▼); $x = 0.05$ (◆); $x = 0.03$ (×), and $x = 0$ (●).

(Figure 4 inset), where all $M(H)$ curves intersect at ~ 18 kOe, and the magnetizations for $Fe[TCNE]_2 \cdot zCH_2Cl_2$ and $V[TCNE]_2 \cdot zCH_2Cl_2$ have the same value. Despite such a behavior, which is characteristic of a physical mixture, detailed analysis reveals that the $M(H)$ curves for each x are not a simple superposition of those for pure compounds. The lack of inflection in $M(H)$ for all solid solutions with $x \geq 0.03$ at low fields rules out the presence of a significant amount of $Fe[TCNE]_2 \cdot zCH_2Cl_2$ expected in any physical mixture. Additionally, in accord with increased disorder, the $M(H)$ at 50 kOe for $x = 0.03$ is substantially suppressed from that expected for the corresponding physical mixture.

The $M(H)$ between ± 1 kOe at 5 K reveals hysteretic behavior for the solid solution of $V_xFe_{1-x}[TCNE]_2 \cdot zCH_2Cl_2$ ($0.1 \leq x \leq 0.9$), Figure 4. The coercivity, H_{cr} , rapidly increases with increasing Fe content (decreasing x), reaching ~ 1120 Oe for $x = 0.03$ (Figure 5). It should be noted that, despite the similar shape of hysteresis curves, the coercivity of $Fe[TCNE]_2 \cdot zCH_2Cl_2$ at low temperatures varies considerably depending upon synthetic route. The material made via almost instantaneous reaction of $FeI_2 \cdot xCH_3CN$ and TCNE has $H_{cr} \approx 2.2$ kOe between 2 and 5 K,¹³ whereas H_{cr} is suppressed to 450 Oe for $Fe[TCNE]_2 \cdot zCH_2Cl_2$ prepared via relatively slow reaction of TCNE and $Fe(CO)_5$. X-ray powder diffraction data indicate that the latter route results in more crystalline material; hence, the higher H_{cr} corresponds to the more disordered compound.

Partial substitution of V^{II} with Fe^{II} in $V[TCNE]_2 \cdot zCH_2Cl_2$ introduces an additional disorder. Therefore, the gradual increase of H_{cr} with increase of x is appar-

ently related to the increase of structural disorder in the solid solutions. The coercivity decreases exponentially upon warming and above 100 K, H_{cr} is $\sim 9 \pm 1$ Oe and becoming essentially temperature-independent for all solid solutions $V_xFe_{1-x}[TCNE]_2 \cdot zCH_2Cl_2$ ($0.1 \leq x \leq 0.9$). Interestingly, at ~ 100 K the inflection in $M(H)$ for $x = 0$ also disappears² suggesting that a macroscopic anisotropy field $H_a(T)$ is totally averaged out above this temperature.

As stated previously, the substitution of Fe^{II} for V^{II} in $V[TCNE]_2 \cdot zCH_2Cl_2$ introduces additional disorder to the material. As a result, the system has a higher degree of randomness in its already amorphous structure, and phase separation is minimized. Because $Fe[TCNE]_2 \cdot zCH_2Cl_2$ prepared from $Fe(CO)_5$ orders at a significantly lower temperature (~ 105 K) than $V[TCNE]_2 \cdot zCH_2Cl_2$, an effective percolation limit (or critical concentration of V) should exist that provides sufficient magnetic coupling on a macroscopic scale to enable a material with high T_c (> 250 K) and magnetic ordering. This model suggests that magnetic ordering at high temperatures requires extended coupling between pairs of V spin sites bridged by a single $S = 1/2$ $[TCNE]^-$.¹⁴ Each $[TCNE]^-$ has four CN groups whose lone pairs are sp-hybridized; therefore, each CN can only bond to one M. Each octahedral V or Fe site most probably bonds to 6 $[TCNE]^-$ molecules. To fulfill the stoichiometry, on average only 3 of the 4 Ns on each $[TCNE]^-$ bond to an M; hence, each M bonds to two additional Ms, resulting

(14) Coupling between V sites solely via $V^{II} \cdots [TCNE]^- \cdots Fe^{II} \cdots [TCNE]^- \cdots V^{II}$ type linkages may be important for low values of x .

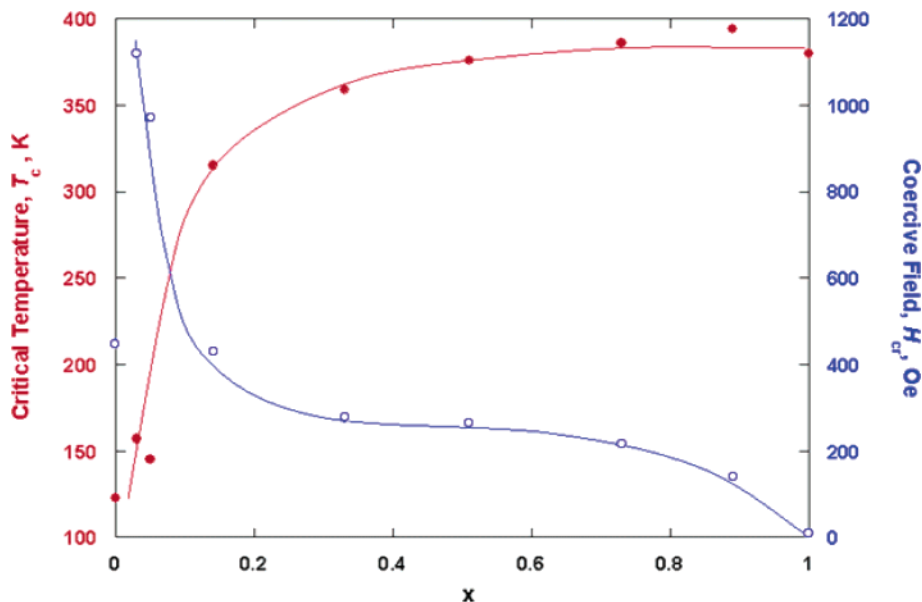


Figure 5. Ordering temperature, T_c (●), and coercivity, H_{cr} (○), as a function of x for $V_xFe_{1-x}[TCNE]_2 \cdot zCH_2Cl_2$ ($0 \leq x \leq 1$); the lines are guides for eyes.

in a total of 12 “nearest neighbor” M sites. Hence, one of the nearest neighbors must be V^{II} if Fe^{II} does not participate in the magnetic ordering above 100 K. The experimental results suggest that the percolation limit is below 0.3, as the onset T_c does not change very much for $x \geq 0.3$. The differences in the shape in $M(T)$ as $T \rightarrow T_c$ are attributed to different concentrations of Fe that are weakly coupled (although more strongly than Co in the analogous systems) to the V-based magnetic cluster.

The spin-glass phase persists through the percolation limit into the magnetically ordered phase.¹² At low temperatures, the magnetic phase breaks into a number of relatively large but randomly frozen sub-clusters, forming a cluster-glass phase. Hence, the long-range magnetic order is destroyed, although magnetic clusters are still present.

The sensitivity of $\chi''(T)$ to magnetic cluster formation supports a “re-entrant” behavior. The first magnetic transition occurs at ~ 340 K for $x \approx 0.5$. $\chi''(T)$ for $V_xFe_{1-x}[TCNE]_2 \cdot zCH_2Cl_2$ has a frequency dependence, suggesting that Fe ions provide a substantial random potential that perturbs the finite magnetic phase. (This is in contrast to $\chi''(T)$ behavior in $V_xCo_{1-x}[TCNE]_2 \cdot zCH_2Cl_2$,⁵ which is almost frequency-independent below the first transition temperature.) However, the $\chi''(T)$ shift per frequency decade is much smaller for $V_xFe_{1-x}[TCNE]_2 \cdot zCH_2Cl_2$ than expected for blocking,^{12c} suggesting a spin-glass phase. $\chi''(T)$ abruptly drops below ~ 120 K, indicating a magnetic transition to a different

state that is probably related to freezing of the magnetization component in the V-based magnetic cluster. Another magnetic transition occurs at ~ 10 K that is related to the freezing of the magnetization component in the Fe subsystem.⁴ This re-entrant behavior has been observed for the amorphous metallic magnets,^{12d} and an increase of the random anisotropy arising from an increase of the iron content leads to the enhanced H_{cr} .

In summary, a family of new solid solution room-temperature magnets of $V_xFe_{1-x}[TCNE]_2 \cdot zCH_2Cl_2$ ($0 < x < 1$) composition has been characterized. Substitution of Fe^{II} for V^{II} in $V[TCNE]_2 \cdot zCH_2Cl_2$ does not significantly alter the T_c for $x \geq 0.3$; however, H_{cr} is enhanced by more than 2 orders of magnitude, indicating a drastic increase of random anisotropy. Hence, the magnetic properties of the room-temperature $V[TCNE]_2 \cdot zCH_2Cl_2$ magnet can be finely tuned via a synthetic chemistry methodology, making this material more amenable to future technologies. Preparation and study of solid-solution thin-film magnets is now in progress.

Acknowledgment. The continued partial support by the Department of Energy Division of Materials Science (grants DE-FG03-93ER45504, DE-FG02-01ER-45931, DE-FG02-86ER45271, and DE-FG02-96ER12198), DARPA through ONR (grant N00014-02-1-0593), and Army Research Office (grant DAAD19-01-1-0562) is gratefully acknowledged.

CM049368B